Investigation of Electromagnetic Bandgap (EBG) Structures for Antenna Pattern Control

Yoonjae Lee[†], Junho Yeo and Raj Mittra*

Electromagnetic Communication Laboratory
319 EE East, The Pennsylvania State University, University Park, PA16802
mittra@engr.psu.edu

[†]Presently with Center for Remote Sensing, Inc.
11350 Random Hills Rd., Suite 710, Fairfax, VA22030

Abstract: In this paper we investigate the use of a variety of EBG structures as components of a number of different antenna designs, with a view to assessing their pattern control capabilities. The EBG configurations investigated include both the one- and two-dimensional geometries comprising of dielectric slabs and rods, as well as air pockets in the dielectric. The antenna types used to investigate the EBG materials are microstrip patch, dielectric resonator (DRA) and tapered slot (TSA) types. We compare the numerical simulation results for the gain patterns of original antennas (no EBG) with those that have EBG materials. The studies show that it is not a trivial task to control the radiation characteristics of planar and three-dimensional antennas, described in this paper, by using EBG structures.

Electromagnetic Bandgap (EBG) materials are periodic structures, which can be designed to impede the propagation of EM waves propagation at certain frequency bands--referred to as the bandgap frequencie--that are determined by the periodicities of the materials and their dielectric constants. Recently, various applications of EBG materials such as microwave filters, antennas, and ground plane structures have been reported in the literature [1-3]. In this work, we investigate the feasibility of EBG materials to tailor the radiation patterns of a number of different antenna configurations. Fig.1 shows the three EBG structures investigated, *viz*., dielectric rods, dielectric slabs, and air pockets in a dielectric material. The dimensions of EBG structures are: rod/slab thickness=3.5mm, rod/slab separation distance=7.876mm, air-pocket thickness=4.376mm, and air-pocket separation distance=7.876mm. A unit cell of periodic structure consists of four dielectric or air constituents and has been simulated for TEM wave propagation assuming PECs for the top and bottom and PMCs for the sides. The bandgap frequencies have been observed at 13GHz, 15GHz, and 17GHz for the three EBG materials. The first antenna investigated is a microstrip patch antenna, shown in Fig. 3. Figure 4 shows the pattern comparison for the antenna with and without the EBG. All patterns are plotted using a 40dB scale. The patch antenna parameters are: width=length=28mm, substrate thickness=3mm (ε_r=10), ground plane size=200mm × 200mm. The EBG substrate is found to affect the back lobes, somewhat, but has little influence on the pattern near the horizon. The next antenna studied is a DRA and Figs 5, 7, and 8 show its configuration with and without the EBGs. Once again the results show that the insertion of the EBG material alters the radiation patterns of the antenna to some extent, but does little to suppress the side lobes. Finally, we analyze a TSA with the same three EBG structures (see Fig. 9). All EBG material has PEC plate on top/bottom and backsides. Because the three EBG structures each have different bandgap frequencies, we show the patterns of the free standing TSA at those frequencies (Figs. 10, 12, and 18) for the sake of comparison. In Figs. 14 and 15, we have plotted the radiation patterns for the case when the antenna has protrusions. Results show that only the dielectric slab EBG exhibits the anticipated behavior, which is the development of nulls at non-propagating directions (Fig. 13). Figure 20 (a) shows the attenuation of the propagating waves through EBG structure, though the same phenomenon is hardly noticeable in (b).

Conclusions

0-7803-7846-6/03/$17.00 ©2003 IEEE

Three types of antenna and EBG structures have been investigated with the objective of altering the sidelobe levels of the antenna. The results have not been as promising as desired and further investigation of ways to combine planar antennas with EBG structures are needed.

References

[1] William J. Chappell, Matthew P. Little, and Linda P. B. Katehi, "High Isolation, Planar Filters Using EBG Structures," *IEEE Microwave and Wireless Components Letters*, Vol. 11, No. 6, pp. 246-248, June 2001.
[2] Cyril Cheype, Cedric Serier, Marc Thevenot, Thierry Monediere, Alain Reineix, and Bernard Jecko, "An Electromagnetic Bandgap Resonator Antenna," *IEEE Transactions on Antennas and Propagation*, Vol. 50, No. 9, pp. 1285-1290, September 2002.
[3] M. M. Sigalas, R. Biswas, Q. Li, D. Crouch, W. Leung, Russ Jacobs-Woodbury, Brian Lough, Sam Nielsen, S. McCalmont, G. Tuttle, and K. M. Ho, "Dipole Antennas on Photonic Bandgap Crystals-Experiment and Simulation", *Microwave and Optical Technology Letters*, Vol. 15, No. 3, pp. 153-158, June 1997.

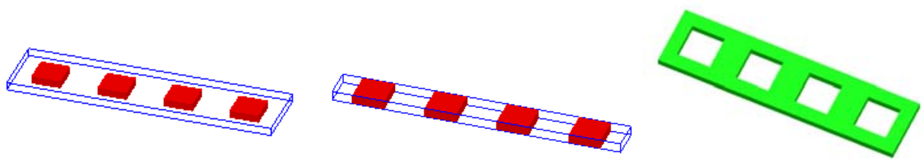

(a) rod (b) slab (c) pocket

Figure 1. One unit cell of EBG materials.

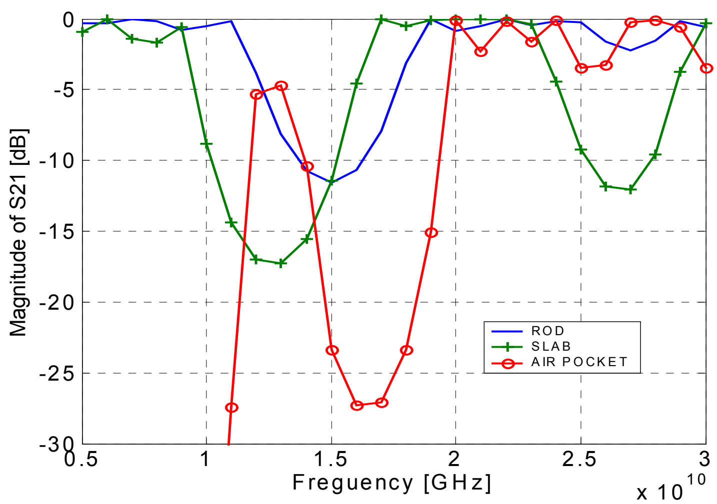

Figure 2. Transmission characteristics of EBG materials.

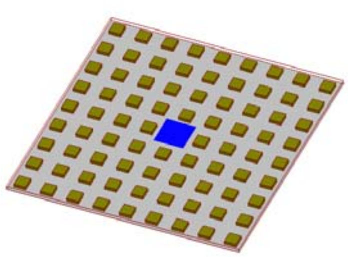

Figure 3. Patch antenna with EBG.

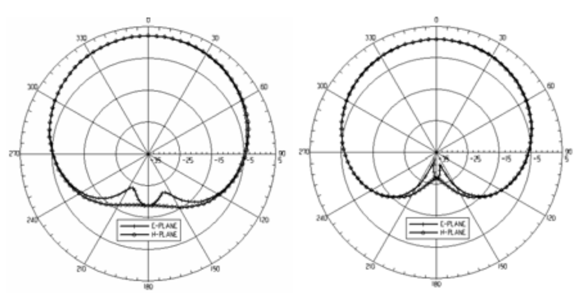

(a) conventional (b) EBG substrate

Figure 4. Comparison of antenna gain pattern.

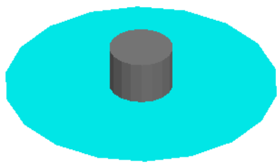

Figure 5. DRA.

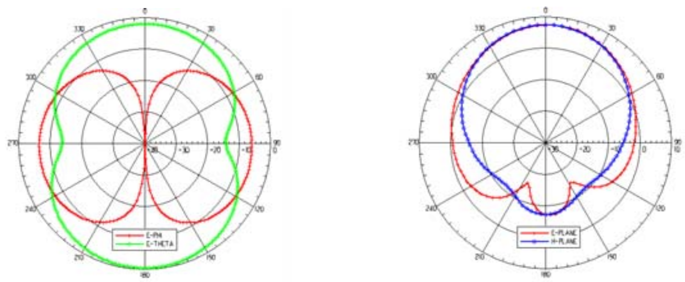

(a) E-theta and E-phi – azimuth (b) Total field – elevation

Figure 6. Gain patterns of DRA.

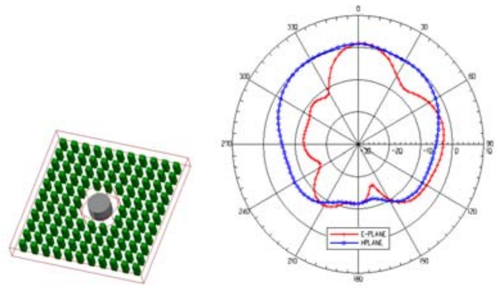

Figure 7. DRA with EBG and its gain pattern.

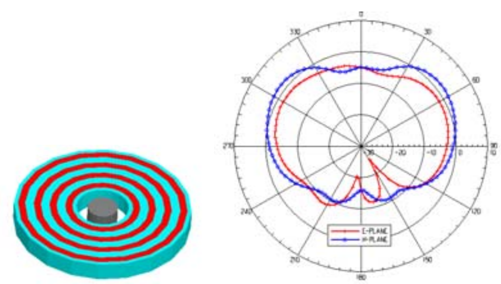

Figure 8. DRA with EBG ring and its gain pattern.

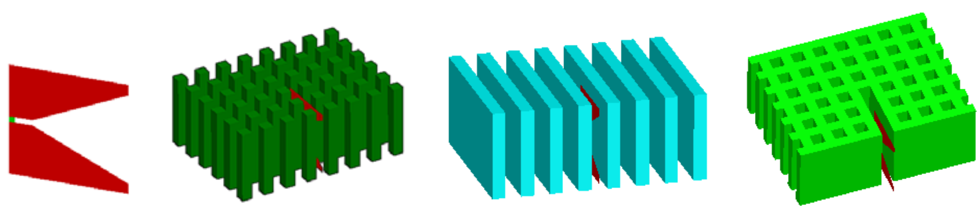

(a) TSA (b) dielectric rods (c) dielectric slabs (d) air pockets

Figure 9. TSA and EBG structures.

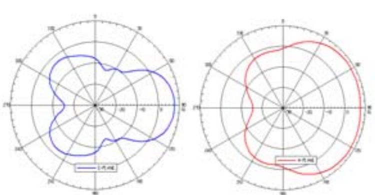

(a) E-plane (b) H-plane

Figure 10. TSA patterns at 15GHz.

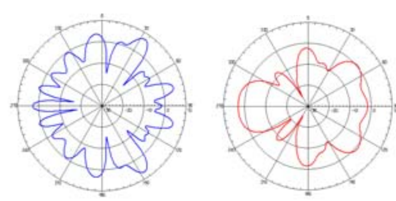

(a) E-plane (b) H-plane

Figure 11. Patterns of TSA with dielectric rods.

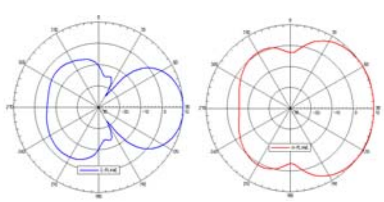

(a) E-plane (b) H-plane

Figure 12. TSA patterns at 13GHz.

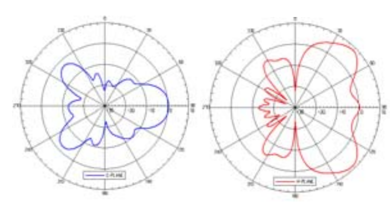

(a) E-plane (b) H-plane

Figure 13. Patterns of TSA with dielectric slabs.

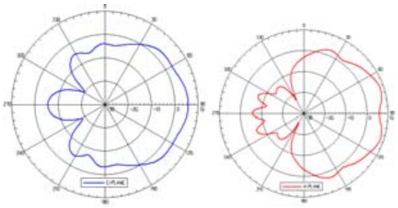

(a) E-plane (b) H-plane

Figure 14. Patterns of TSA with dielectric slabs. (5mm protrusion)

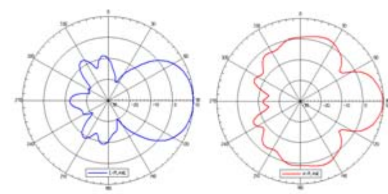

(a) E-plane (b) H-plane

Figure 15. Patterns of TSA with dielectric Slabs. (10mm protrusion)

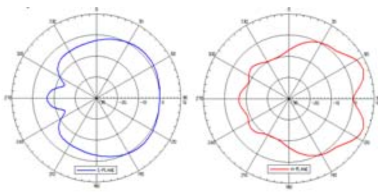

(a) E-plane (b) H-plane

Figure 16. Patterns of TSA with dielectric slabs with side PEC.

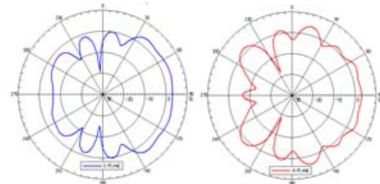

(a) E-plane (b) H-plane

Figure 17. Patterns of TSA with dielectric slabs without back PEC.

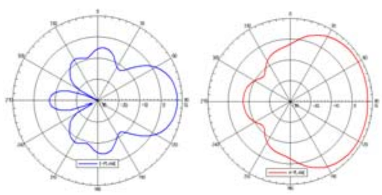

(a) E-plane (b) H-plane

Figure 18. Patterns of TSA pattern at 17GHz.

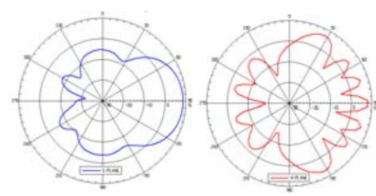

(a) E-plane (b) H-plane

Figure 19. Patterns of TSA with air-pocket EBG.

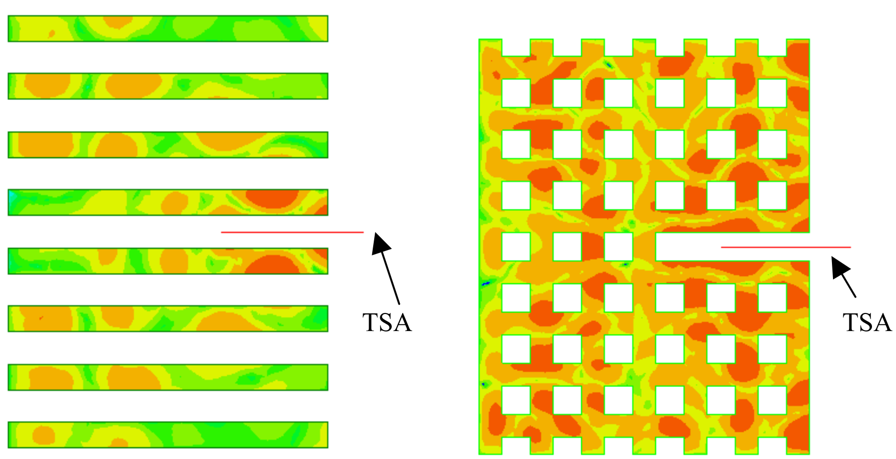

(a) dielectric slab EBG (b) air pocket EBG

Figure 20. Comparison of E-field distribution.